Quantitative Functional Group Orientation in Langmuir Films by Infrared Reflection−Absorption Spectroscopy: C═O Groups in Behenic Acid Methyl Ester and *sn*2-^{13}C-DSPC

Joseph W. Brauner,[†] Carol R. Flach,[†] Zhi Xu,[†] Xiaohong Bi,[†] Ruthven N. A. H. Lewis,[‡] Ronald N. McElhaney,[‡] Arne Gericke,[§] and Richard Mendelsohn*,[†]

Department of Biochemistry, University of Alberta, Edmonton, Alberta, Canada T6G2H7, Department of Chemistry, Kent State University, Kent, Ohio 44242, and Department of Chemistry, Newark College of Arts and Science, Rutgers University, 73 Warren Street, Newark, New Jersey 07102

Received: January 16, 2003; In Final Form: May 9, 2003

IR reflection−absorption spectroscopy (IRRAS) is used to determine the orientation of carbonyl groups in behenic acid methyl ester (BME) and in *sn*2-^{13}C 1,2 distearoylphosphatidylcholine (*sn*2-^{13}C-DSPC) in aqueous monolayer films. The C═O stretching contour of BME consists of three overlapped peaks arising from unhydrated, monohydrated, and doubly hydrated forms at 1737, 1721, and 1702 cm^{-1}, respectively. Dichroic ratios constructed from the p- and s-polarized IRRAS intensities of the resolved components of the contour were simulated with the optical theory of V. L. Kuzmin.[1,2] On the basis of valence bond and molecular modeling considerations, the carbonyl group is essentially perpendicular to the chain axes. The transition moment is determined by IRRAS to indeed lie along the C═O bond for the unhydrated groups (thus providing good support for the theory) but changes direction for hydrated groups. A satisfactory fit between simulation and experiment could not be obtained by assuming a uniaxial distribution of the zigzag all-trans methylene chain to which the carbonyl group is rigidly attached. A slight preferential orientation of the chain planes in the direction perpendicular to that of the trough barrier movement is found for both BME and *sn*2-^{13}C DSPC. In addition, spectral quality in the 1000−1300 cm^{-1} region for BME was sufficient to determine that the orientation of the single-bond C−O stretch of the ester moiety was within 20° of the vertical. For *sn*2-^{13}C-DSPC, each C═O bond stretching contour was split into a doublet arising from hydrated and unhydrated forms. The best fit to the IRRAS data for the unhydrated C═O mode in each chain led to a suggested chain tilt of 30°. This value, in good accord with X-ray diffraction measurements,[3] was confirmed through analysis of the CH_2 stretching vibrations. The transition moments of the hydrated C═O bonds in *sn*2-^{13}C-DSPC were again found to not lie along the bond direction. The current analysis provides a new method for determining functional group orientation in monolayers. The approach, when coupled with X-ray and neutron reflectivity measurements, will provide unique information about the structures and interactions of film constituents.

Introduction

Infrared reflection−absorption spectroscopy (IRRAS), developed by Dluhy and co-workers in the mid-1980s,[4,5] provides a unique means of acquiring molecular structure information from lipid/protein monolayer (Langmuir) films in situ at the air−water interface. Two types of spectral information result from IRRAS measurements: frequencies and intensities. Frequencies are easier to interpret, and they provide information in the usual way about molecular structure and interactions. As an example, initial applications of IRRAS were mostly confined to qualitative determination of lipid acyl chain conformational order, as deduced from the chain CH_2 stretching frequencies.[6,7] These are sensitive to chain *trans*−*gauche* isomerization. Very specific information about chain packing may occasionally be acquired from the CH_2 scissoring vibrations (1460−1475 cm^{-1}), which split into a doublet with components near 1462 and 1474 cm^{-1} if the chains pack in an orthorhombic perpendicular fashion.[8,9] Such a doublet has been observed for Langmuir films of behenic acid methyl ester (BME).[10]

In addition to the acyl chain modes providing information about conformational order and packing, the frequencies of the polar headgroup vibrations reflect its environment and interactions with the subphase. For example, Gericke and Hühnerfuss deduced the hydration state of C═O bonds from their stretching frequencies in fatty acid films.[11]

Since the initial experiments on Langmuir films of lipids, IRRAS technology has improved to the point where good quality spectra of proteins in lipid monolayers may be acquired.[12,13] The most useful information about protein structure comes from Amide I frequencies (mostly peptide bond C═O stretch) which are well correlated with protein secondary structures. Several summaries of IRRAS applications to the study of Langmuir films have recently appeared.[14−17]

The second, less widely used aspect of IRRAS involves the determination of chain and functional group orientation from quantitative evaluation of measured band intensities. Several IRRAS studies have determined acyl chain orientation (as a mean tilt from the surface normal) in ordered phospholipid[12] and fatty acid monolayer films.[18] In general, the observed results

* To whom correspondence should be addressed. Phone 973-353-5613; Fax 973-353-1264; E-mail mendelso@andromeda.rutgers.edu.
[†] Rutgers University.
[‡] University of Alberta.
[§] Kent State University.

10.1021/jp030066r CCC: $25.00
Published on Web 06/25/2003

are consistent with those derived from X-ray scattering measurements. Recently, the Rutgers group has used an improved IRRAS apparatus to show that different acyl chain tilt angles occur in each chain of a fatty-acid homogeneous derivative of ceramide 2.[19] This experiment, which has no counterpart in X-ray reflection, required an isotopically labeled derivative of ceramide 2 in which one of the chains was perdeuterated, thus shifting its methylene vibrations into a spectral region free from interference by other vibrational modes.

In addition to determination of chain orientation, a few IRRAS studies have also reported the orientation of proteins in mixed Langmuir films with phospholipids. For example, the orientation of the helical pulmonary surfactant protein SP−C in monolayers of 1,2-dipalmitoylphosphatidycholine (DPPC) was derived. At a surface pressure of ∼30 mN/m, the helix was shown to be tilted at ∼70° from the surface normal.[20] A polarization−modulation (PM)-IRRAS study reported qualitative pressure-dependent orientation for gramicidin A in mixed lipid−peptide monolayers.[13]

A unique aspect of IRRAS intensity measurements yet to be substantially exploited is determination of the orientation of isolated functional groups in fatty acids and phospholipids. The most intense functional group vibrations likely to be useful in this regard are acid or ester C═O stretching modes (∼1700−1750 cm^{-1}). Several factors complicate the measurement of these bands on an aqueous subphase. These modes occur in a spectral region where liquid water, most commonly used as the subphase, distorts the spectral background, while water vapor in the optical path produces very sharp rotation−vibration absorption bands between ∼1400−1900 cm^{-1}. The former problem may be eliminated through use of a D_2O subphase, while water vapor interference may be eliminated either by use of a sample shuttle[14,21] or through PM-IRRAS techniques.[22] An additional complication in the study of phospholipids is that the observed carbonyl bands are comprised of overlapped vibrations from the C═O groups of both the *sn*1 and *sn*2 chains. Finally, the geometric models used to determine the optical constants needed for theoretical simulation of the IRRAS bands have in the past assumed a uniaxial distribution.[23] This assumption had to be discarded in the present work.

The current study approaches the problem of C═O orientation in Langmuir films through studies of BME and *sn2*-^{13}C═O 1,2-distearoylphosphatidylcholine (*sn2*-^{13}C-DSPC). The choice of the BME was based on previous observations that the chains are perpendicular to the monolayer plane, thus eliminating one unknown (chain tilt) in the theoretical analysis.[10,24] The choice of *sn2*-^{13}C-DSPC is based on biophysical interest, PC's constituting an important lipid class in membranes and in pulmonary surfactant. The isotopically labeled derivative is needed to produce different frequencies for the *sn*1 and *sn*2 C═O vibrational modes. The molecular structures of BME and *sn*2-^{13}C-DSPC are given in Figure 1.

Experimental Section

Materials. Chloroform, EDTA, and HPLC-grade water were obtained from Fisher Scientific (Pittsburgh, PA). BME (99% pure), trizma [2-amino-2-(hydroxymethyl)-1,3-propanediol] hydrochloride, and sodium chloride were purchased from Sigma (St. Louis, MO). D_2O with 99.9% isotopic enrichment was purchased from Cambridge Isotope Laboratories (Andover, MA).

*Sn*2-^{13}C-DSPC was prepared as described in detail elsewhere.[25] Briefly, the molecule was synthesized by the 4-pyrrolidinopyridine-catalyzed acylation of 1-*O*-stearoyl lyso-PC

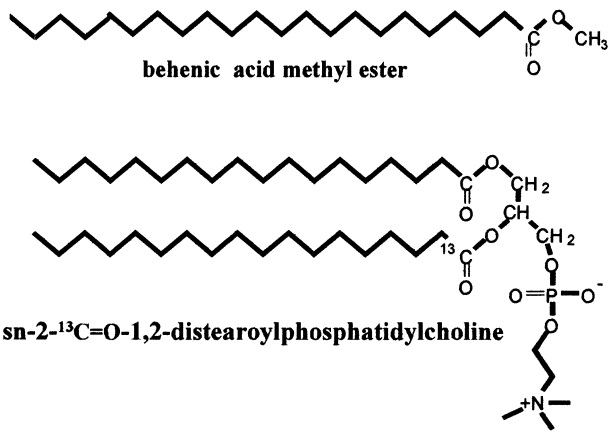

Figure 1. Structures of behenic acid methyl ester (BME) and of *sn*2-^{13}C 1,2-distearoyl-phosphatidylcholine (*sn*2-^{13}C-DSPC).

(Avanti Polar Lipids, Alabaster, AL), using an excess of the 1-^{13}C fatty acid anhydride (^{13}C enrichment = 99%, MSD Isotopes, Montreal, Canada). A 700 mg amount of the labeled fatty acid was dissolved in CCl_4 and 1 g of *N*,*N*′-dicylcohexylcarbodiimide (DCC) was added. The mixture was shaken at room temperature for 1 h, after which the precipitated *N*,*N*′-dicyclohexyl urea was removed by filtration. Following removal of solvent under a stream of N_2 gas, the residue (fatty acid anhydride and excess DCC) was stirred at 45 °C and the catalyst was added (0.1 mol/mol of fatty acid) in 0.5 mL of benzene, followed by a slurry of 100 mg of the lyso-PC in 2 mL of $CHCl_3$. After stirring at 45 °C for 3 h, the reaction mixture was diluted with $CHCl_3$, applied to a silicic acid column, and purified as described previously. ^{13}C NMR analysis of the product showed that no more than 3% acyl chain migration occurred.

IRRAS/Langmuir Trough Accessory. The IRRAS equipment has been described in detail previously.[19] Briefly, spectra were acquired with a Bruker Instruments, Equinox 55 Spectrometer equipped with an external variable angle reflectance accessory (Bruker model XA511). The accessory is a self-contained computer-controlled unit attached to the external port on the spectrometer coupled to a custom-designed Langmuir trough with a Nima model PS4 surface pressure sensor (Nima Technologies, Coventry, England). The IR beam is directed through the external port in the spectrometer and is reflected by three mirrors in a rigid mount prior to being focused on the water surface. Computer-driven stepper motors rotate the mirrors to obtain the desired angle of incidence. An IR polarizer is placed into the optical path just prior to the beam impinging on the water surface. The reflected light is collected at the same angle as the angle of incidence, follows an equivalent symmetric mirror path, and is directed onto the narrow band MCT detector. For accurate simulations, polarizer efficiency must also be known. Unlike transmission spectroscopy, where a slight (<2%) polarizer leak will not seriously alter the measured intensities, a small amount of s-polarized radiation leaking into the p-channel may seriously alter the derived orientation information. Polarizer efficiency was determined to be about 99.2%.

The entire experimental setup is enclosed and purged to keep the relative humidity levels both low and as constant as feasible. A sample shuttle, driven by a computer-controlled stepper motor, allows interferograms from the reference side (aqueous surface) and from the sample side (film-covered surface) to be collected in alternating fashion. The number and size of co-added interferogram blocks can be varied to provide a high signal-to-noise ratio and to most efficiently compensate for water vapor.

IRRAS Sample Preparation and Spectral Acquisition. A D_2O-based subphase consisting of 150 mM NaCl and 0.1 mM EDTA in 5 mM Tris buffer at pD 6.9 was used for all experiments involving analysis of the carbonyl band. An equivalent buffer in HPLC water was used as the subphase for experiments where other lipid headgroup vibrational modes were investigated. A 10−20 μL amount of lipid solution in organic solvent ($CHCl_3$) was spread dropwise on the surface (maximum surface area of 86 cm^2) of the trough; 30 min was allowed for solvent evaporation and film relaxation/equilibration. Films were continuously compressed at a speed of ∼0.02 nm^2/molecule-min while surface pressure−molecular area (π−A) isotherms were recorded. When the desired surface pressure was reached (∼35 mN/m for BME and ∼40 mN/m for *sn*2-^{13}C-DSPC), the films were again allowed to relax for at least 30 min. prior to IR data collection. Surface pressure decreased slightly (≤5 mN/m) during this time period. A time delay of 35 s was allowed for film equilibration between trough movement and data collection. Typically, blocks of 1024 scans were collected for the BME and *sn*2-^{13}C-DSPC monolayers at all angles of incidence. There were 8192 scans required to achieve good S/N ratios for the 1000−1300 cm^{-1} region of *sn*2-^{13}C-DSPC. Interferograms were collected at ∼8 cm^{-1} resolution, co-added, apodized with a Blackman−Harris-3-term function, and fast Fourier transformed with one level of zero-filling to produce spectral data encoded at ∼4 cm^{-1} intervals. Spectra were acquired over the desired range of incident angles using p-polarized radiation followed by data collection using s-polarized light. IRRAS spectra were baseline corrected using Grams/32 software (Galactic Industries). Peak positions were determined using a center of gravity algorithm provided by the National Research Council of Canada. Curve-fitting routines were developed in house.

Theory

Polarized IRRAS spectra of the carbonyl groups in monolayers of BME and *sn*2-^{13}C-DSPC on D_2O have been simulated with the reflectance equations from the optical theory (see the Appendix) of V. L. Kuzmin and his associates,[1,2] which apply to a thin layer (film) between two semi-infinite phases. The spatial orientation of the C═O groups in these molecules can be obtained by matching simulated and experimental IRRAS dichroic ratios as will be explained below. The theory requires knowledge of the optical constants (index of refraction, *n*, and extinction coefficient, *k*) of all three layers as well as the film thickness.

The first semi-infinite phase is air, which is isotropic, practically nonabsorbing, and has an index of refraction of essentially 1. The second semi-infinite phase is D_2O, which is also taken to be isotropic and whose indices of refraction and extinction coefficients in the 1650−1750 cm^{-1} region are taken from Bertie's data.[26] Although the isotropic nature of the D_2O subphase in the vicinity of the surface may deviate due to hydration of monolayer constituents, the thickness of this layer is unknown and the absorption bands of D_2O are not in the wavenumber regions under study in the current work. The film was taken to be anisotropic with distinct values for the three Cartesian components of its optical constants in the laboratory frame. Previous analyses of films on various surfaces have assumed a uniaxial molecular distribution,[10,20] but, in this instance, the Cartesian components of the extinction coefficients calculated from Fraser's equations for uniaxial systems[23] cannot produce complete agreement between simulated and experimental dichroic ratios.

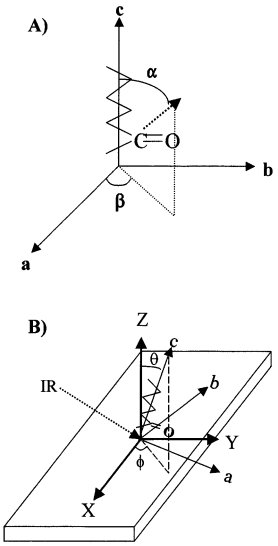

Figure 2. (A) Local *abc* and (B) laboratory *XYZ* coordinate systems used in the IRRAS spectral simulations of BME and DSPC at the air−water interface. The infrared beam is in the *YZ* plane, and θ and Φ are the polar and azimuthal angles of the local *c* axis in the laboratory frame. The acyl chain is shown as a zigzag line with a C═O group rigidly attached to the chain. α and β describe the transition moment of the C═O bond in the molecule fixed system.

To obtain the components of the extinction coefficient of the film in the laboratory frame, a right-handed Cartesian coordinate system (displayed in Figure 2) is selected such that the positive *Z* axis is along the surface normal, the *X* axis is in the direction of the film barrier movement in the Langmuir trough, and the *YZ* plane is the plane of incidence. A local right-handed Cartesian coordinate system, *abc*, is attached to the acyl chains such that the *c* axis is in the direction of the all-trans acyl chain with the positive sense as up from the headgroup, the *a* axis is in the plane of the carbon skeletal backbone and has the same sense as the C═O bond vector which also lies in this plane, and the *b* axis is perpendicular to the plane of the zigzag carbon backbone.

The orientation of the local system in the laboratory frame is described by the Euler angles, θ, φ, and χ, as defined in Wilson et al.[27] The orientation of the C═O transition moment in the laboratory frame has only two degrees of freedom, so that only θ and φ, the ordinary polar and azimuthal angles of the *c* axis in the laboratory frame, need to be determined. Molecular rotation around the *c* axis, χ, was fixed at 0 degrees. The orientation of the transition moment vector, *M*, associated with the C═O stretch in the local system is described by a polar angle α and an azimuthal angle β. In this case

$$k_X = (m_a \cos\theta \cos\varphi - m_b \sin\varphi + m_c \sin\theta \cos\varphi)^2 \quad (1)$$

$$k_Y = (m_a \cos\theta \sin\varphi + m_b \cos\varphi + m_c \sin\theta \sin\varphi)^2 \quad (2)$$

$$k_Z = (-m_a \sin\theta + m_c \cos\theta)^2 \quad (3)$$

where $m_a = M \sin\alpha \cos\beta$, $m_b = M \sin\alpha \sin\beta$, and $m_c = M \cos\alpha$. The magnitude of *M* depends on the oscillator strength of the C═O stretching mode.

In simulating a particular IRRAS band, a Lorentzian wavenumber distribution of total extinction coefficients having an appropriate center frequency, amplitude, and bandwidth is assumed. The amplitude is adjusted to match the intensity of

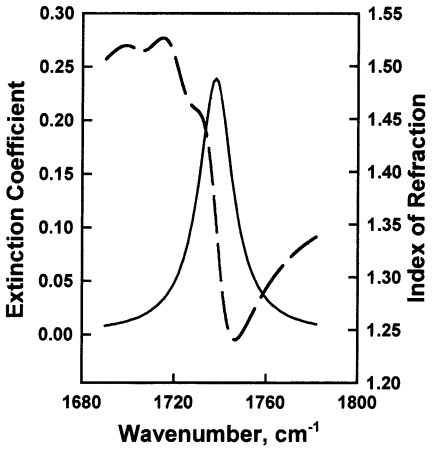

Figure 3. Lorentzian wavenumber distribution of the extinction coefficient of the 1737 cm^{-1} band of BME (—) and the behavior of the index of refraction in this region for all three bands in the BME C═O region (---) are depicted. The simulations require the index of refraction to be a summed contribution from all of the bands that contribute to the dispersion in the wavenumber range.

the calculated band to that of the experimental band. This accounts for the magnitude of *M*. The values so obtained are typical of monolayer films. The values of the Cartesian components of the extinction coefficients are governed by the angular parameters described above.

The total index of refraction of the film in the vicinity of absorption bands is related to the total extinction coefficient since these are, respectively, derived from the real and imaginary parts of the solution of the equation of motion for a damped harmonic oscillator in a sinusoidal electric field. The same parameters used in the extinction coefficient calculation are used in the complex index of refraction calculation for a given band. When dealing with overlapped bands, such as those produced by hydrated and unhydrated versions of a carbonyl group, and nearby bands, such as those due to ^{12}C and ^{13}C carbonyls in the same molecule, a term for each of the bands present must be included in the index of refraction calculation since their anomalous dispersion effects overlap. This effect is depicted in Figure 3.

Results

BME. Typical s- and p-polarized IRRAS spectra at several angles of incidence for the C═O stretching region (1600−1850 cm^{-1}) of BME on D_2O are shown in Figure 4. The C═O stretching region consists of three components at 1737, 1721, and 1702 cm^{-1}, which have been attributed to free, singly hydrogen-bonded, and doubly hydrogen-bonded C═O groups, respectively.[11] The free C═O band, the most intense in the contour, was analyzed first since its transition moment is anticipated to lie along the CO bond. Both elementary bonding considerations and a molecular mechanics analysis show this bond to be essentially perpendicular to the chain, so that α is 90° and β is 0° (see Figure 2). Therefore, only θ and ϕ remain to be determined.

The C═O contours for BME in the two polarizations at a number of angles of incidence below the Brewster angle were resolved and the area for each component quantified by curve fitting. Three bands were required, as discussed above. The areas of the individual s- and p-polarized components of the 1737 cm^{-1} peak are plotted as a function of angle of incidence in Figures 5A and B, respectively. In each case, the experimental areas are compared with those calculated for assumed values

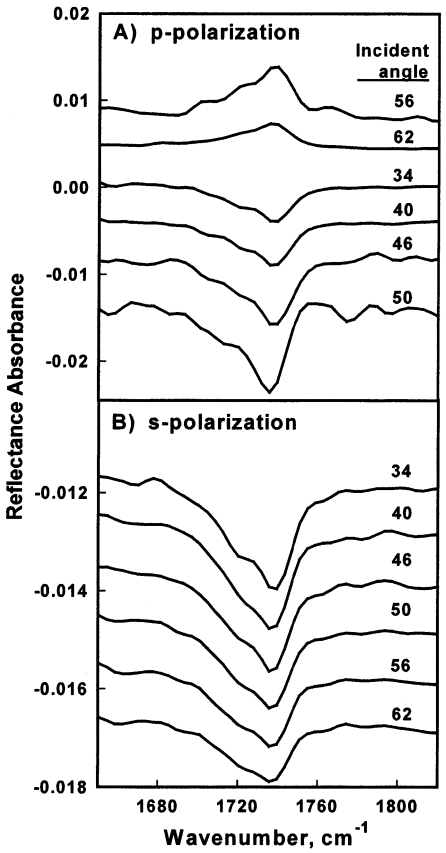

Figure 4. Experimental IRRAS spectra of the C═O region of BME: (A) p-polarization and (B) s-polarization. The angles of incidence are noted.

of *K*, which is a scale factor that determines the amplitude of the real and imaginary parts of the refractive index. The calculated intensities are evidently strongly dependent on *K*. These calculations assumed uniaxial symmetry. A more detailed analysis (see below) showed that these conditions, while approximately true, were not exactly met for the current films. The strong dependence of the IRRAS band areas on *K* makes it difficult to determine the best values of α and β for bands in which these are unknown. To eliminate this problem, a standard technique from IR-ATR spectroscopy was employed, namely, the use of dichroic ratios. The experimental and calculated intensities are plotted (Figure 5C) as p/s area ratios, as a function of angle of incidence. The theoretical dichroic ratios, plotted as lines in Figure 5C, are five overlapped curves (essentially indistinguishable from one another), corresponding to the set of *K* values used in Figures 5A and 5B. Thus, the calculated dichroic ratio is essentially independent of the value of *K*, within a range reasonable for thin films. Likewise, dichroic ratios are not sensitive to an assumed film thickness, thereby eliminating another source of uncertainty. It is evident from the figure that although the agreement between the theoretical curves and experimental points is reasonable, there appears to be a small systematic deviation between experimental and theoretical values. The systematic error was traced to breakdown of the assumption of uniaxial symmetry. To illustrate this, the experimentally determined dichroic ratios for the 1737 cm^{-1} band were plotted in Figure 6A as points vs angle of incidence superimposed on the calculated values generated from Kuzmin's equations[1,2] but using eqs 1−3 to generate the optical constants, thereby eliminating the molecular orientation averaging normally assumed for uniaxial symmetry. The simulated results are shown as lines where the extinction coefficient components depend

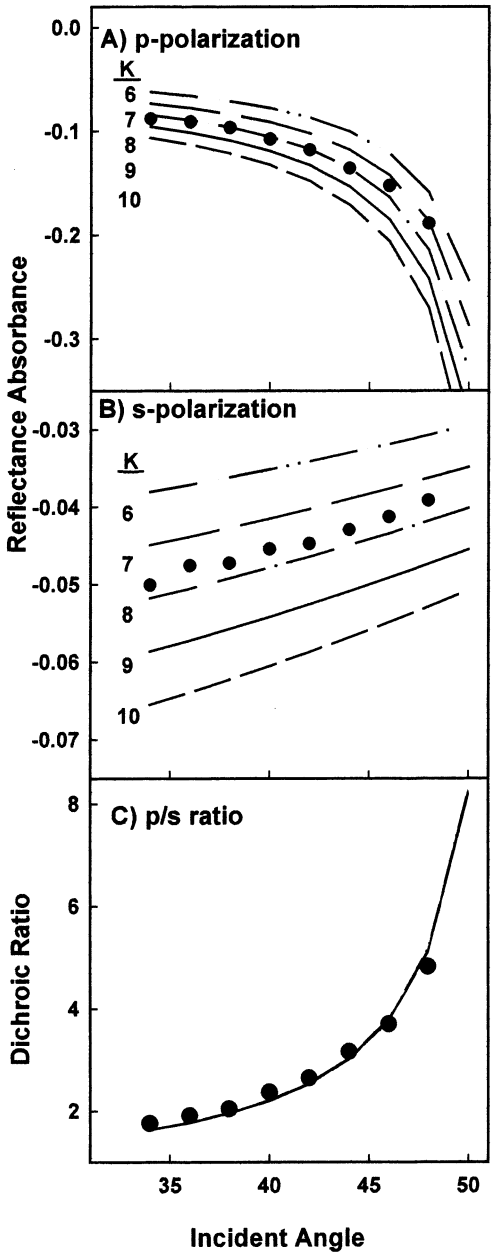

Figure 5. Dependence of IRRAS band intensities on scale factor (*K*) for the 1737 cm^{-1} component of the C═O contour in BME is demonstrated in (A) for p-polarization and (B) for s-polarization. The experimental data points are filled circles and lines representing simulated results at various *K* values as noted. In each case, the choice of *K* causes large changes, which obscure the much smaller effects of altered α, the tilt of the C═O transition moment with respect to the chain axis. However, when the p/s dichroic ratio is plotted as shown in part C, the effects of changing *K* are largely mitigated. (C) Calculated curves for all *K* values are essentially overlapped.

on θ and φ. The best fit was obtained for $\theta = 0°$ and $\varphi = 46.5°$. The result for θ is consistent with previous studies from this laboratory[10] and confirmed elsewhere,[24] both of which show that the BME chain has a 0° tilt. The result for φ suggests that the plane of the zigzag carbon backbone has a slight preferential alignment in the *Y* direction. Random alignment would have resulted in $\varphi = 45°$ rather than the best fit value of 46.5°.

The sensitivity of the simulated dichroic ratio to φ is also shown in Figure 6A for values of $\varphi = 45°$ and 48°. Changes of more than ~1° evidently make a large difference in the calculated ratio and result in an easily seen departure from the experimental points. The precision of the current experimental

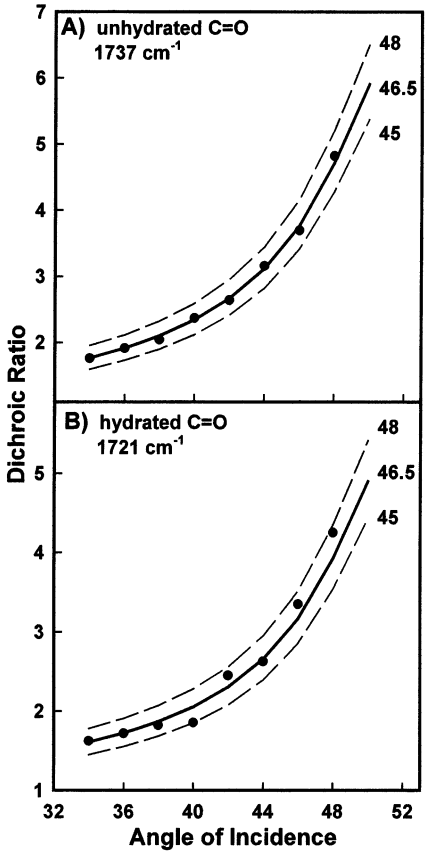

Figure 6. Effects of including deviations from uniaxial symmetry in the calculations of functional group orientation. A comparison of experimental (filled circles) and theoretical (lines) dichroic ratios for Φ values from 45° to 48°. For the unhydrated C═O band of BME depicted in part A, the following parameters were used: $\alpha = 90°$, $\beta = 0°$, and $\theta = 0°$. For the singly hydrated C═O depicted in part B, the parameter set used was $\alpha = 61°$, $\beta = 0°$, and $\theta = 0°$. The best fit between simulated values and experimental data for both bands was found using $\Phi = 46.5°$.

data thus places reasonable constraints on the quantitative determination of the deviation from uniaxial symmetry.

The C═O band at 1721 cm^{-1} arising from singly hydrated C═O species was analyzed next. The experimental dichroic ratios for this feature, as plotted in Figure 6B, are clearly different (~10−20% smaller) from those for the 1737 cm^{-1} band shown in Figure 6A. The observed experimental differences in p/s intensity ratios must arise from different transition moment directions (i.e., α and β) for the hydrated vs the unhydrated C═O group. The α and β values cannot be deduced from simple geometric considerations, as was the case for the 1737 cm^{-1} component of the contour (since the H bond is likely to alter the transition moment direction from its initial value along the bond direction), and hence constitute previously unavailable information. The best fit, shown in Figure 6B, was obtained for $\alpha = 61°$ and $\beta = 0°$. Evidently, monohydration rotates the transition moment ~30° from the C═O bond in the plane of the all-trans carbon backbone while leaving the azimuthal angle unchanged. Finally, the third band in the contour, arising from the doubly hydrated C═O species at 1702 cm^{-1}, could not be analyzed quantitatively because of its low intensity.

As an independent check on the new methodology established here, the entire IRRAS contour was simulated from the sum of the three individual components as described above. One comparison between the experimental and simulated spectra (for

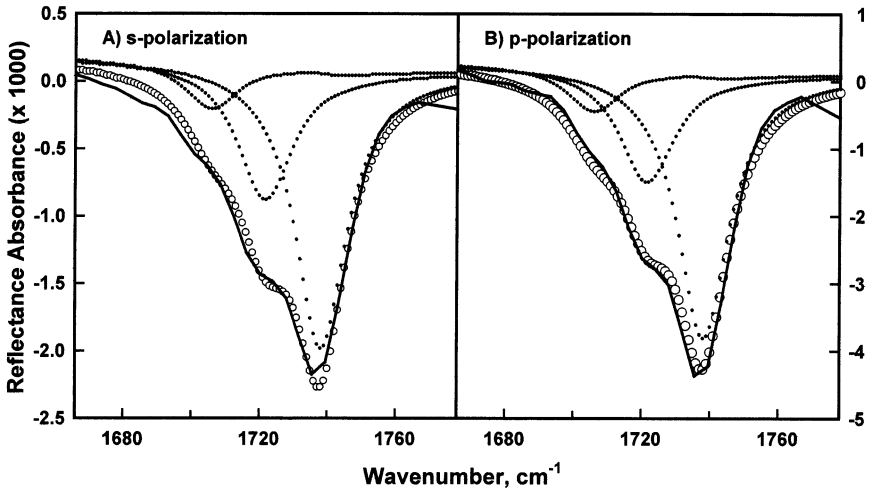

Figure 7. Fit between (A) s-polarized and (B) p-polarized experimental IRRAS spectra for the C═O stretching region of BME and the simulated bands generated from Kuzmin's theory. The experimental spectra are represented by the solid lines, the underlying simulated bands by dotted lines, and the sum of the simulated bands by open circles.

an angle of incidence of 34°) is shown in Figure 7 for s and p polarization. The agreement is seen to be quite good for both polarizations.

DSPC. The carbonyl region of the IRRAS spectra (1620−1800 cm^{-1}) of *sn*2-^{13}C-DSPC is shown for s- and p-polarized radiation at several angles of incidence in Figure 8A and B. This spectral region shows two main bands at 1739 and 1693 cm^{-1}, arising from the *sn*1 (^{12}C) and *sn*2 (^{13}C) C═O groups, respectively. Each of these peaks is asymmetric, indicating the presence of overlapped bands, which, in each case, can be resolved into a doublet, the former with components at 1739 and1729 cm^{-1} and the latter with components at 1693 and 1683 cm^{-1}. The higher frequency component of each doublet has been assigned to an unhydrated C═O bond, while the lower frequency component has been assigned to a hydrated C═O group.

The two component bands for the unhydrated carbonyls at 1693 and 1739 cm^{-1} were analyzed first. As for BME, the C═O bond (unhydrated state) was taken to lie in the plane of the all-trans carbon backbone and to be perpendicular to the chain direction. The transition moment for these bands is assumed to lie along the C═O bond, which makes $\alpha = 90°$ and $\beta = 0°$. The plot for the p/s intensity ratio vs angle of incidence for each of the unhydrated C═O's is shown in Figure 9A and C; the best fit is obtained for both bands with $\theta = 30°$ and $\varphi = 49°$. As for BME, the φ result shows a preferential alignment of the plane of the all-trans carbon backbone in the *Y* direction, with a preference slightly larger than that for BME.

In this instance, the value of θ is subject to independent verification through analysis of the CH_2 stretching vibrations. IRRAS spectra of the CH_2 stretching region for the molecule as a function of angle of incidence for s- and p-polarized radiation are shown in Figure 10. The chain orientation was determined as previously described,[10] using Fraser's equations for uniaxial symmetry.[23] Experimental intensities for the symmetric CH_2 stretching vibration are compared with calculated values for s and p polarization in Figure 11 for tilt angles of 25°, 30°, and 35°. The best value for acyl chain tilt is seen to be ∼30° with an uncertainty estimated to be ±1−2°. For reasons discussed elsewhere, values derived for experimental angles of incidence less than the Brewster angle are considered to be more reliable.[10]

For analysis of the hydrated C═O stretching bands at 1683 and 1729 cm^{-1}, θ was kept at 30° and φ at 49°. Under these conditions, good fits in the dichroic ratio plots (Figure 9B and

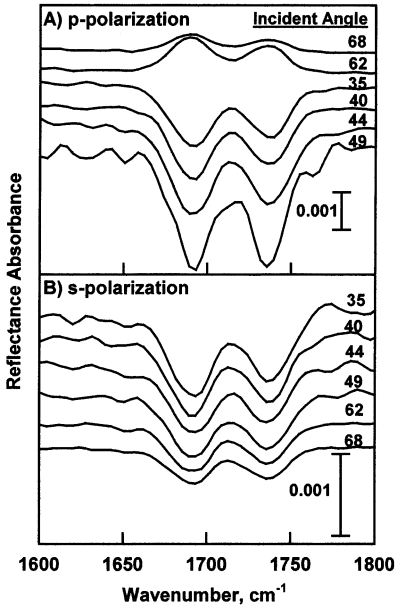

Figure 8. Experimental IRRAS spectra of the C═O stretching region for *sn*2-^{13}C-DSPC at different angles of incidence using (A) p-polarized and (B) s-polarized radiation.

D) are obtained with $\alpha = 50°$ and $\beta = -10°$. The sensitivity to changes in β over the range −20° to 0° is high, but the sensitivity to changes in α is reduced for modes with the preponderance of their transition moment intensities in the *XY* plane. Thus, a range of α values gives almost equally good fits to the data. An additional source of uncertainty arises because the experimental dichroic ratios for DSPC have more scatter than comparable data for BME (Figure 6), presumably because of greater uncertainties in curve fitting the experimental contours, which are more overlapped and less intense than for BME.

As an additional independent check on the procedures established here, the entire IRRAS contour was simulated from the sum of the four individual components as described above. One comparison between the experimental and simulated spectra (for an angle of incidence of 48°) is shown in Figure 12 for p polarization. The agreement is seen to be good.

Orientation of the C−O Bond in BME. In addition to the orientation of the C═O bonds, the current experimental data for BME are sufficiently good to make some semiquantitative

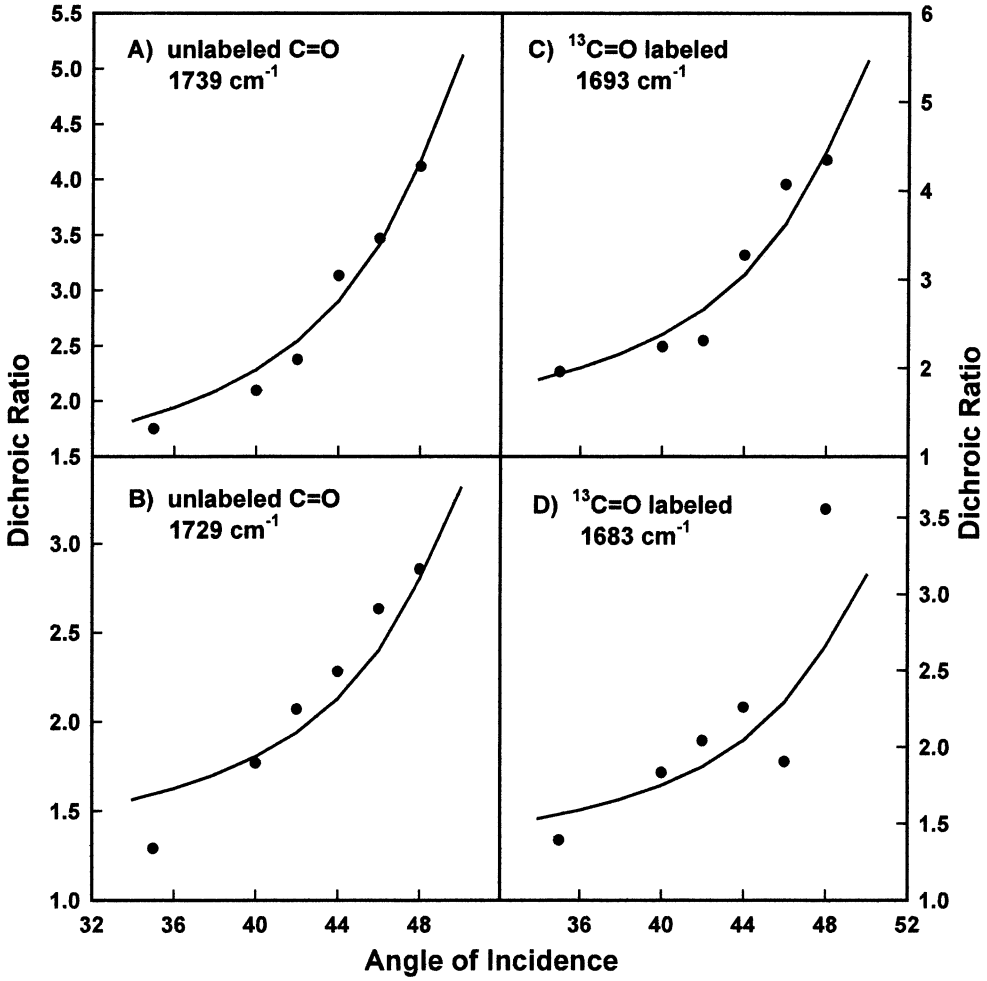

Figure 9. Experimental (closed circles) and simulated best fit (lines) dichroic ratios over a range of angles of incidence for the unhydrated and singly hydrated C═O stretching bands of *sn*2-^{13}C-DSPC as follows: (A) unhydrated C═O stretch at 1739 cm^{-1} for the unlabeled *sn*1 chain, with parameters $\alpha = 90°$, $\beta = 0°$, $\theta = 30°$, and $\phi = 49°$; (B) hydrated C═O stretch at 1729 cm^{-1} for the unlabeled *sn*1 chain, with parameters $\alpha = 50°$, $\beta = -10°$, $\theta = 30°$, and $\phi = 49°$; (C) unhydrated C═O stretch at 1693 cm^{-1} for the labeled *sn*2 chain, with parameters $\alpha = 90°$, $\beta = 0°$, $\theta = 30°$, and $\phi = 49°$; and (D) hydrated C═O stretch at 1683 cm^{-1} for the labeled *sn*2 chain, with parameters $\alpha = 50°$, $\beta = -10°$, $\theta = 30°$, and $\phi = 49°$.

statements about the orientation of transition moments giving rise to other vibrations in the 1000−1300 cm^{-1} region. Spectral data acquired with s- and p-polarized radiation at several angles of incidence away from the Brewster angle are shown in Figure 13. Most interesting is the observation of the band at 1178 cm^{-1} arising from the sp^2 ester C−O single-bond stretching mode from the $CH_2CO-OCH_3$ fragments. The band has little or no intensity in the s-polarized spectra, which suggests that the C−O transition moment is perpendicular to the *XY* plane. Spectra acquired with p-polarized radiation are consistent with this, as a positive-going (negative-going) C−O band is observed at incident angles less than (greater than) the Brewster angle. Simulated p and s bands for this mode for a range of α values are shown in Figure 14. Values in the 0−20° range adequately bracket the experimentally observed spectral data and thus set limits on the orientation of the C−O transition moment.

Discussion

The current experiments demonstrate both the feasibility and technical difficulties of determining tilt angles for individual functional groups in aqueous Langmuir films. The importance of the problem lies in the fact that no other current technology can provide this information, which will define elements of the three-dimensional structure of the monolayer constituents. Whereas X-ray techniques and IRRAS each provide acyl chain tilt angles from ordered chains, IRRAS alone can detect individual bond orientations, with some assumptions possibly required about the relationship between transition moment and bond directions. The approach should also be applicable to the study of disordered phases, where the utility of X-ray techniques is limited.

Some comments about the new methodology established here are in order. The prior observations that the BME chains are perpendicular to the monolayer surface[10,24] remove one variable from the formalism used here and provide the means to assess the validity of the current theoretical approach. In addition, the suggestion that $\alpha = 90°$ for the C═O bond, a value derived from simple geometric models, provides a testable prediction, which in fact produces excellent accord between calculated and experimental dichroic ratios. Improvement is achieved when the assumption that the two in-plane directions are not exactly equivalent ($\varphi = 46.5°$ rather than 45° for equivalence) is included in the calculation.

The origin of nonequivalence in the *XY* plane is of some interest generally in the physics of monolayers. In the current instance, we believe it is derived from the fact that the monolayers are compressed along a particular direction. However, more fundamental cases have been described in the X-ray literature. Dutta discussed the fact that, for some phases of fatty acids, the chains cannot be represented as cylinders.[28] He noted

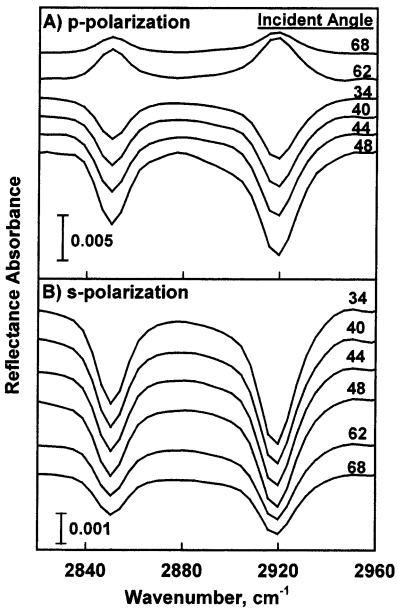

Figure 10. Experimental (A) p-polarized (B) s-polarized IRRAS spectra of the CH_2 stretching region of *sn*2-^{13}C-DSPC at various angles of incidence.

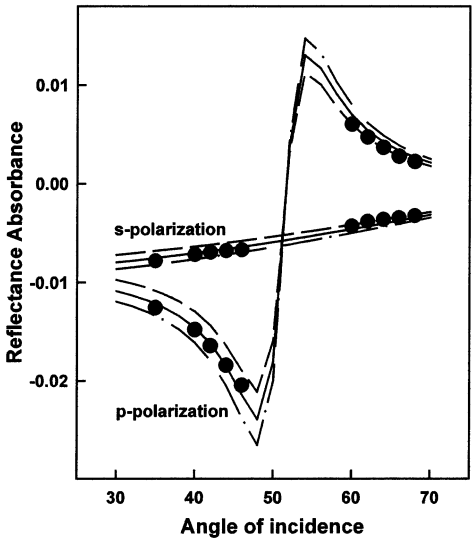

Figure 11. Calculated (lines) and experimental (filled circles) data for the symmetric CH_2 stretching mode (2850 cm^{-1}) for *sn*2-^{13}C-DSPC at various angles of incidence for tilt angles of 25° (dash−dot), 30° (solid), and 35° (dashed) for s- and p-polarization. Data below the Brewster angle are considered more accurate than those above. The best derived value for the chain tilt angle is 30° ± 1° or 2°.

that to fully specify molecular arrangements, the orientational distribution of the molecule about its long axis must be determined and summarized how X-ray diffraction intensities may be used to study backbone ordering. Such effects have not been previously reported for functional groups.

Recently Lösche and colleagues presented a new approach to X-ray analysis, which provides some insight into headgroup conformation and hydration.[29] They showed that upon the LE → LC transition in dimyristoylphosphatidic acid (DMPA), changes in headgroup orientation are coupled to acyl chain ordering. In particular, the average orientation of the headgroup fragment (determined from the projected distance between both acyl chain carbonyls and the phosphate group) tilts away from the interface in going to the LC phase. As the headgroup is increased in size toward phosphatidylcholine, it is unclear

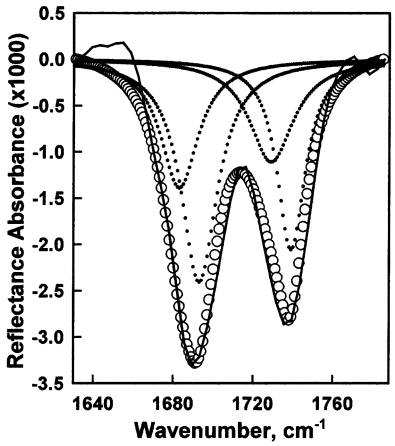

Figure 12. Fit between p-polarized experimental IRRAS spectra for the C═O stretching contour (angle of incidence = 48°) and the simulated bands generated from Kuzmin's theory using the parameters reported in the text. The experimental spectrum is represented by the solid lines, the underlying simulated bands by dotted lines, and the sum of the simulated bands by open circles.

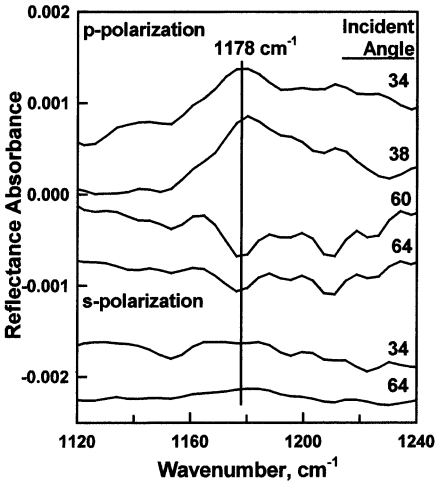

Figure 13. p- and s-polarized IRRAS spectra for the C−O stretching region of BME at angles of incidence as noted.

whether the ordering events observed for DMPA will continue to be strongly coupled. In this instance, IRRAS measurements will be quite helpful, in view of the ability of the method to determine transition dipole orientation of particular functional groups whose bond directions in the molecular framework are known.

There is a small amount literature addressing similar problems in the bulk phase. Nagle suggested, from a comparison of attenuated total reflectance (ATR)-IR and X-ray measurements, that in stacked bilayers of phospholipids a preferential rotational order of hydrocarbon chains about their long axis may be present.[30] For instance, in gel-phase DPPC, there is a preference for the plane defined by the chain carbons to be more perpendicular than parallel to the plane defined by the tilt direction and the bilayer normal. In our geometry, this acyl chain plane would correspond to the local "*cb*" plane.

There are also very limited bilayer data for functional group orientation that may be pertinent to the current results for comparison purposes. Hubner and Mantsch used polarized ATR−IR to examine oriented multilayers of *sn*2-^{13}C-1,2 dimyristoylphosphatidylcholine and *sn*2-^{13}C-1,2 dipalmitoyl-phosphatidylcholine.[31] They calculated the direction of the transition moment of the C═O bond relative to the bilayer normal to be greater than about 64° and 66° for the *sn*-1 and

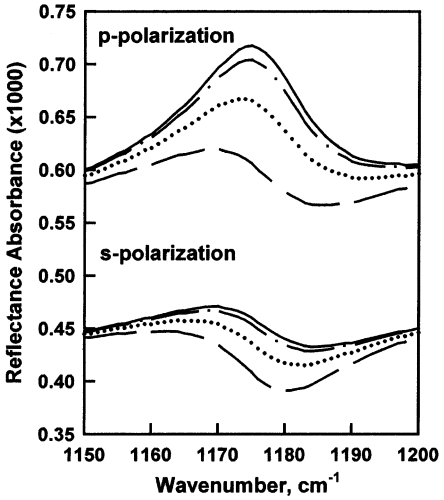

Figure 14. Simulated p- and s-polarized IRRAS spectra of the C−O stretch for BME as α is varied from 0°, 10°, 20°, and 30° from top to bottom in each instance. Other parameters are $\beta = 0°$, $\theta = 0°$, $\phi = 45°$, and angle of incidence = 34°.

sn-2 chains, respectively, at $T < T_m$,. However, Hubner and Mantsch made no attempt to differentiate the hydrated from the unhydrated C═O modes of the individual bonds.

The current analysis, which was directed primarily toward developing a method for determination of functional group orientation, in addition provided new information about the transition moments of the hydrated component of the C═O contour in both BME and DSPC. The band components that arise from singly H-bonded species had their transition moment direction shifted as a consequence of H-bond formation. Examination of structural parameters from X-ray studies of hydrated C═O groups[32,33] leads to a possible model. An angle of approximately 120° is reported between the C═O carbon and the H-bonded hydrogen atom of water in the crystal ($\angle_{C=O\cdots H} \approx 120°$). In addition, a nearly linear relationship exists between the carbonyl oxygen and bonded H−O in water ($\angle_{O-H\cdots O} \approx$ linear). From these parameters a reasonable model can be envisioned in which the transition moment of the (hydrated) C═O stretching vibration would point toward the direction of the oxygen atom of the hydrating water molecule rather than along the bond.

For DSPC, the C═O bond orientation in both the *sn*1 and *sn*2 chains was assumed to be 90° relative to the chain axis. This assumption leads to a calculated chain tilt of 30°, in excellent agreement with the chain tilt independently derived from IRRAS analysis of the chain methylene vibrations and from the X-ray diffraction measurements.[3] Hydration of the C═O produces changes in the direction of the transition moment in the local frame, although uncertainties in the curve fitting lead to some ambiguity in the determination.

Finally, it is relevant to comment on the general feasibility of IRRAS for determination of functional group orientation. First, there is sufficient experimental precision in the data for BME (Figures 4 and 6) to evaluate the sensitivity of the p/s ratio to selected values of α or ϕ and to judge that the optical model of Kuzmin[1,2] is appropriate over the complete range of transition moment directions and angles of incidence. Second, deviations from uniaxial symmetry need to be incorporated into the analysis. As the number of measurements of functional group orientation increases, it will be useful to combine these orientations with X-ray and/or neutron studies of lipid monolayers to approach a three-dimensional determination of lipid structure in Langmuir films.

Acknowledgment. This work was supported from NIH grant (PHS-GM-29864) to R.M., Term Operating grant from the Canadian Institutes of Health to R.N.M., and NIH grant (PHS-AR-38910-15) to A.G.. Professors R.A. Lalancette and H. W. Thompson are thanked for useful discussions.

Appendix

Several parameters are required to calculate a single RA value. These are the mean tilt angle of the molecular axis relative to the surface normal, θ, the angle that the transition dipole makes with the molecular axis, α, vacuum wavelength of the light, λ, film thickness, h, indices of refraction and extinction coefficients of the incident and final phases, n_0, n_2, k_0, k_2, the index of refraction of the film, n, and the directional extinction coefficients of the film, k_x, k_y, and k_z. The reflection coefficients of a thin anisotropic film have been given by Kuzmin and associates[1,2] as follows, where the tilde indicates a complex quantity.

For s polarization

$$\tilde{r}_s = -\frac{\sin(\varphi_1 - \tilde{\varphi}_2) - ik_0\tilde{n}_2^{-1}\sin\varphi_1\tilde{I}_x}{\sin(\varphi_1 + \tilde{\varphi}_2) - ik_0\tilde{n}_2^{-1}\sin\varphi_1\tilde{I}_x} \tag{4}$$

For p polarization

$$\tilde{r}_p = \frac{\sin(\varphi_1 - \tilde{\varphi}_2)\cos(\varphi_1 + \tilde{\varphi}_2) - ik_0\tilde{n}_2^{-1}\sin\varphi_i(\tilde{I}_y\cos\varphi_1\cos\tilde{\varphi}_2 - \tilde{I}_2\sin\varphi_1\sin\tilde{\varphi}_2)}{\sin(\varphi_1 + \tilde{\varphi}_2)\cos(\varphi_1 - \tilde{\varphi}_2) - ik_0\tilde{n}_2^{-1}\sin\varphi_i(\tilde{I}_y\cos\varphi_1\cos\tilde{\varphi}_2 + \tilde{I}_2\sin\varphi_1\sin\tilde{\varphi}_2)} \tag{5}$$

in which φ_1 is the angle of incidence between the incoming ray and the direction of the surface normal, φ_2 is the complex angle of the refracted ray, and $k_0 = 2\pi/\lambda$. In the current application, we use the ratio of p/s-polarized intensity to compare the experimental with the simulated peaks, since use of the ratio eliminates the necessity to have a very accurate scale factor (K). Although the calculated s and p curves individually show a strong dependence on K, the p/s ratio does not.

In cases (the most common situation) where the variation in the optical properties of the film in the z direction is unknown

$$\tilde{I}_x = (\tilde{n}_x^2 - \tilde{n}_2^2)h,\ \tilde{I}_y = (\tilde{n}_y^2 - \tilde{n}_2^2)h, \text{ and } \tilde{I}_2 = \frac{(\tilde{n}_z^2 - \tilde{n}_2^2)}{\tilde{n}_z^2}h \tag{6}$$

where the complex refractive index, $\tilde{n}_c = n + ik_c$ with $c = x$, y, or z, n is the real part of the refractive index, and k_c is the directional extinction coefficient for the film. The complex refractive index for the subphase is given by $\tilde{n}_2 = n_2 + ik_2$.

The Lorentzian band shape for k is given by $k_i = wK/(4(\upsilon_i - \upsilon_0)^2 + w^2)$ in which w is the width, K is a scale factor, υ_0 is the center frequency, and the subscript i refers to the ith wavenumber. Finally, $n_i = 1.41 - \sum_j(\upsilon_i - \upsilon_{0,j})2K/(4(\upsilon_i - \upsilon_{0,j})^2) + w^2$ where the summation is taken over all the subbands.

The reflectivity values, R and R_0, are calculated by multiplying the respective reflection coefficients with their complex conjugates so that RA values measured in IRRAS experiments are obtained. These reflectance−absorbance values are compared with experiment.

References and Notes

(1) Kuzmin, V. L.; Michailov, A. V. *Opt. Spectrosc. (USSR)* **1981**, *51*, 383.
(2) Kuzmin, V. L.; Romanov, V. P.; Michailov, A. V. *Opt. Spectrosc.* **1992**, *73*, 1.
(3) Brezesinski, G.; Müller, H. J.; Toca-Herrera, J. L.; Krustev, R. *Chem. Phys. Lipids* **2001**, *110*, 183.
(4) Dluhy, R. A.; Cornell, D. G. *J. Phys. Chem.* **1985**, *89*, 3195.
(5) Dluhy, R. A. *J. Phys. Chem.* **1986**, *90*, 1373.
(6) Mitchell, M. L.; Dluhy, R. A. *J. Am. Chem. Soc.* **1988**, *110*, 712.
(7) Hunt, R. D.; Mitchell, M. L.; Dluhy, R. A. *J. Mol. Struct.* **1989**, *214*, 93.
(8) Snyder, R. G. *J. Mol. Spectrosc.* **1960**, *4*, 411.
(9) Snyder, R. G. *J. Mol. Spectrosc.* **1961**, *7*, 116.
(10) Flach, C. R.; Gericke, A.; Mendelsohn, R. *J. Phys. Chem.* **1997**, *101*, 58.
(11) Gericke, A.; Hühnerfuss, H. *J. Phys. Chem.* **1993**, *97*, 12899.
(12) Bi, X.; Taneva, S.; Keough, K. M. W.; Mendelsohn, R.; Flach, C. R. *Biochemistry* **2001**, *40*, 13659.
(13) Ulrich, W.-P.; Vogel, H. *Biophys. J.* **1999**, *76*, 1639.
(14) Mendelsohn, R.; Flach, C. R. Infrared reflection−absorption spectrometry of monolayer films at the air−water interface. In *Handbook of Vibrational Spectroscopy*; Chalmers, J. M., Griffiths, P. R., Eds.; John Wiley and Sons, Ltd.: Chichester, UK, 2002; Vol. 2, p 1028.
(15) Mendelsohn, R.; Flach, C. R. Infrared reflection−absorption spectroscopy of lipid, peptides, and proteins in aqueious monolayers. In *Current Topics in Membranes: Peptide-Lipid Interactions*; Simon, S. A., McIntosh, T. J., Eds.; Academic Press: San Diego, 2002; Vol. 52, p 57.
(16) Dluhy, R. A.; Stephens, S. M.; Widayati, S.; Williams, A. D. *Spectrochim. Acta, Part A* **1995**, *51*, 1413.
(17) Blaudez, D.; Buffeteau, T.; Desbat, B.; Turlet, J. M. *Curr. Opin. Colloid Interface Sci.* **1999**, *4*, 265.
(18) Blaudez, D.; Buffeteau, T.; Castaings, N.; Desbat, B.; Turlet, J. M. *J. Chem. Phys.* **1996**, *104*, 9983.
(19) Flach, C. R.; Xu, Z.; Bi, X.; Brauner, J. W.; Mendelsohn, R. *Appl. Spectrosc.* **2001**, *55*, 1060.
(20) Gericke, A.; Flach, C. R.; Mendelsohn, R. *Biophys. J.* **1997**, *73*, 492.
(21) Flach, C. R.; Brauner, J. W.; Taylor, J. W.; Baldwin, R. C.; Mendelsohn, R. *Biophys. J.* **1994**, *67*, 402.
(22) Blaudez, D.; Buffeteau, T.; Cornut, J. C.; Desbat, B.; Escafre, N.; Pezolet, M.; Turlet, J. M. *Appl. Spectrosc.* **1993**, *47*, 869.
(23) Fraser, R. D. B.; MacRae, T. P. *Conformation in Fibrous Proteins and Related Synthetic Polypeptides*; Academic Press: New York, 1973.
(24) Pelletier, I.; Bourque, H.; Buffeteau, T.; Blaudez, D.; Desbat, B.; Pézolet, M. *J. Phys. Chem. B* **2002**, *106*, 1968.
(25) Lewis, R. N. A. H.; McElhaney, R. N. *Biophys. J.* **1992**, *61*, 63.
(26) Bertie, J. E.; Ahmed, M. K.; Eysel, H. H. *J. Phys. Chem.* **1989**, *93*, 2210.
(27) Wilson, E. B.; Decius, J. C.; Cross, P. C. *Molecular Vibrations. The Theory of Infrared and Raman Vibrational Spectra*; McGraw-Hill: New York, 1955.
(28) Dutta, P. *Colloids Surf. A* **2000**, *171*, 59.
(29) Schalke, M.; Krüger, P.; Weygand, M.; Lösche, M. *Biochim. Biophys. Acta* **2000**, *1464*, 113.
(30) Nagle, J. F. *Biophys. J.* **1993**, *64*, 1110.
(31) Hübner, W.; Mantsch, H. H. *Biophys. J.* **1991**, *59*, 1261.
(32) Thompson, H. W.; Lalancette, R. A. *Acta Crystallogr.* **2001**, *C57*, 841.
(33) Lalancette, R. A.; Brunskill, A. P. J.; Thompson, H. W. *Acta Crystallogr.* **1997**, *C53*, 1838.